Supplementary Material:

Methanol-based fixation is superior to buffered formalin for next-generation sequencing of clinical cancer samples

Anna M. Piskorz*, Darren Ennis*, Geoff Macintyre*,
Teodora E. Goranova, Matthew Eldridge, Nuria Segui-Gracia, Mikel Valganon,
Aoisha Hoyle, Clare Orange, Luiza Moore, Mercedes Jimenez-Linan, David Millan,
Iain A. McNeish#, James D. Brenton#

This supplementary document has been generated using *sweave*. The document has an associated sourcecode file which contains a mix of latex and R which when compiled generates the pdf. Each figure in this document is generated dynamically during compilation. For clarity, the code which generates each of these plots is hidden. This code can be accessed by looking at the sourcecode which can be found in the following repository https://bitbucket.org/britroc/fixation. A description of how to reproduce the entire analysis associated with the manuscript can be found at the end of this document. Patient sequencing data can be accessed via application through the European Genome Archive, accesssion EGAS00001001433.

1 Samples

Tissue samples were collected from 16 women (median age 62) with HGSOC undergoing debulking surgery at Glasgow Royal Infirmary, Glasgow, UK. 7/16 samples were acquired at primary debulking surgery, the remaining 9 following 3 - 4 cycles of carboplatin and paclitaxel chemotherapy (summarised in Supplementary Table 1). All samples were collected under the auspices of NHS Greater Glasgow and Clyde Biorepository following approval by West of Scotland Research Ethics Committee 4 (Reference 10/S0704/60). All samples were reviewed by at least two pathologists. Small samples (approximately $20mm^3$) of both tumour and normal tissue were macrodissected, divided into three equal fragments, and fixed in 10% neutral-buffered formalin (Genta Medical, York, UK), UMFIX (Sakura Finetek, Thatcham, UK) or snap frozen (liquid nitrogen). In addition, separate three or more 16G core biopsies (Argon Medical Devices, Athens, TX, USA) of the main tumour mass were taken from 12 cases. After 24 hours, UMFIX and NBF-fixed samples were processed in a Thermo Excelsior Tissue Processor using optimised protocols (Supplementary Table 2 and 3). NBF/UMFIX-fixed normal sample pairs (tumour cells less than 10%) were used only for IHC analysis as controls. A summary of all sample details can be found in Supplementary Table 7.

Supplementary Table 1: Clinical patient information: This table summarises relevant clincial information for the 16 patients included in this study. * - no biopsy cores, IPS - Immediate primary surgery, DPS - Delayed primary surger

Patient ID	Age	Debulking status	Malignant Tissue Type	Normal Tissue	Stage
P5	48	IPS	Ovary	Fallopian Tube	3C
P3	56	IPS	Ovary	Fallopian Tube	3C
P16	69	IPS	Ovary	Fallopian Tube	3A2
P13	82	DPS	Ovary	Uterus	3C
P9	57	IPS	Ovary	Cervix	2A
P11	71	DPS	Omental deposit	Fallopian Tube	3C
P6	53	DPS	Ovary	Myometrium	3C
P15	68	DPS	Omental deposit	Fallopian Tube	3C
P14	57	DPS	Ovary	Uterus	3C
P8	72	IPS	Ovary	Uterus	3A
P4	48	DPS	Ovary	Uterus	4A
P12	65	DPS	Omental deposit	Terminal ileum	4A
P7*	71	IPS	Ovary	Uterus	3C
P10*	68	DPS	Ovary	Myometrium	4B
P2*	56	IPS	Ovary	Uterus	3C
P1*	58	DPS	Vaginal lump	Myometrium	3C

Supplementary Table 2: UMFIX processing cycle: This table contains experimental details for universal molecular fixative processing protocol carried out in this study.

Reagent	Time (mins)	Temperature	Drain	Vacuum	Agitation
70% Ethanol	35	$32/40\,^{\circ}$C	60	Yes	5
90% Ethanol	40	$32/40\,^{\circ}$C	60	Yes	5
95% Ethanol	45	$32/40\,^{\circ}$C	60	Yes	5
100% Ethanol	50	$32/40\,^{\circ}$C	60	Yes	5
100% Ethanol	50	$32/40\,^{\circ}$C	60	Yes	5
100% Ethanol	55	$32/40\,^{\circ}$C	60	Yes	5
Xylene	45	$32/40\,^{\circ}$C	60	Yes	5
Xylene	50	$32/40\,^{\circ}$C	60	Yes	5
Xylene	60	$32/40\,^{\circ}$C	120	Yes	5
Wax	70	$61\,^{\circ}$C	120	Yes	5
Wax	80	$61\,^{\circ}$C	120	Yes	5
Wax	100	$61\,^{\circ}$C	120	Yes	5

Supplementary Table 3: NBF processing cycle: This table contains experimental details for neutral buffered formalin processing protocol carried out in this study.

Reagent	Time (mins)	Temperature	Drain	Vacuum	Agitation
10% NBF	30	$Amb/40\,^{\circ}$C	60	Yes	5
70% Ethanol	35	$32/40\,^{\circ}$C	60	Yes	5
90% Ethanol	40	$32/40\,^{\circ}$C	60	Yes	5
95% Ethanol	45	$32/40\,^{\circ}$C	60	Yes	5
100% Ethanol	50	$32/40\,^{\circ}$C	60	Yes	5
100% Ethanol	50	$32/40\,^{\circ}$C	60	Yes	5
100% Ethanol	55	$32/40\,^{\circ}$C	60	Yes	5
Xylene	45	$32/40\,^{\circ}$C	60	Yes	5
Xylene	50	$32/40\,^{\circ}$C	60	Yes	5
Xylene	60	$32/40\,^{\circ}$C	120	Yes	5
Wax	70	$61\,^{\circ}$C	120	Yes	5
Wax	80	$61\,^{\circ}$C	120	Yes	5
Wax	100	$61\,^{\circ}$C	120	Yes	5

2 Immunohistochemistry

Five μm sections were cut from available surgical samples, biopsies and control samples and were stained for Cytokeratin 7 (CK7), p53, PAX8, WT1 and CK20 on a fully automated Leica Bond III (Leica Microsystems (UK), Milton Keynes, UK) using established clinical protocols in the Department of Pathology, Queen Elizabeth University Hospital Glasgow, with appropriate positive and negative controls. Staining for WT1 on UMFIX tissue was subsequently optimised on a Dako Autostainer (CRUK Beatson Institute, Glasgow, UK). For WT1, antigen retrieval ($98\,^{\circ}$C, 45 minutes, citrate buffer (pH 9)) was followed by 5 minutes endogenous peroxidase block (3% H2O2). Primary antibody was added for 60 minutes at $25\,^{\circ}$C. Antibody binding was visualized using DAB (3-39 diaminobenzidine). Details of antibodies used and dilutions are found in Supplementary Table 4.
Stained slides were digitised (Hamamatsu NanoZoomer NDP, Hamamatsu Photonics, Welwyn Garden City, UK) and viewed using Slidepath Digital Image Hub V4.0.7 (Leica Microsystems, Milton Keynes). Areas of tumour were identified and scored using Slidepath Tissue Image Analysis and histoscores generated by multiplying intensity of cellular staining within marked areas (range 0-3) by percentage cells with positive staining (range 0-100), with a maximum histoscore of 300. Data were analysed using GraphPad Prism version 6.0 (GraphPad software, San Diego, California, USA) - Spearman rho was used to correlate UMFIX and NBF histoscores, and paired t-test used for pairwise histoscore comparisons. All analyses were two-tailed.

Supplementary Table 4: Immunohistochemical assays conditions: This table contains details on the antibodies and systems used for IHC.

Antibody	Clone	Dilution	Manufacturer	Product Number
p53	D0-7	1:300	Leica Biosystems	PA0057
WT1	WT49	1:30	Leica Biosystems	NCL-L-WT1-562
CK7	RN7	1:200	Leica Biosystems	CK7-OVTL-R-7-CE
Pax8	PAX8R1	1:40	Abcam	Ab53490
CK20	PW31	1:100	Leica Biosystems	PA0022

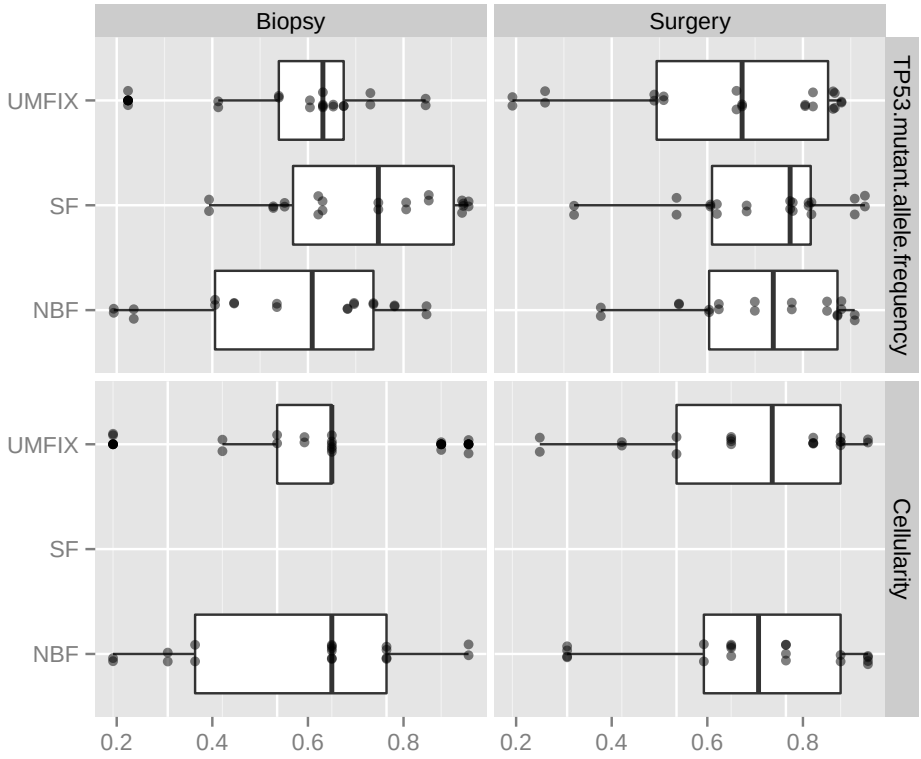

Supplementary Figure 1: TP53 mutant allele frequency and pathology estimated tumour cellularity: Boxplots show the distribution of weighted average TP53 mutant allele frequencies generated across TAm-Seq replicates (66 samples, 11 patients, top) and pathology estimated tumour cellularities (66 samples, 11 patients, bottom)

3 Pathology

Tumour cellularity was assessed by pathologist based on H&E staining performed for all fixed (UMFIX, NBF) biopsy and surgical samples (see Supplementary Table 6 and Supplementary Figure 1). The cellularity was determined as a percentage of tumor cells occupied selected for microdissection area. The microdissected areas were subjected to DNA extraction. Additionally the tumour cellularity was assessed on molecular level using TP53 mutant frequency calculated using TAmSeq data as a proxy.

4 DNA extraction

DNA was extracted from 10-60 sections (10μm thickness) of UMFIX/NBF-fixed tissues using QIAmp DNA Micro kit (Qiagen) with the following modification to the original protocol: an additional incubation step with Buffer ATL at $95\,^{\circ}$C for 15 minutes was introduced before adding proteinase K. Paraffin was removed by the standard xylene/ethanol method. DNA from SF tissues was extracted using AllPrep DNA/RNA Micro Kit (Qiagen) according to the manufacturer's recommendations.

5 DNA quantification and quality assessment

DNA quantification of all samples was performed by Qubit 2.0 Fluorometer (Life Technologies) using dsDNA BR Assay. DNA size distributions were analysed on the Agilent 2100 Bioanalyzer (Agilent Technologies) using the DNA 12000 Kit. All DNA samples were analysed in triplicate and all reactions were performed using the supplier's protocols.

5.1 qPCR of 90bp fragments using Illumina FFPE QC Kit (Illumina)

Results for quantification of 90bp fragments are summarised in Supplementary Figure 2. According to Illumina's recommendations, samples analysed by Illumina FFPE QC Kit that show $\Delta Cq \leq 2.0$ should be suitable for NGS preparation. All but two samples were above this threshold.
Statistical test: The Wilcoxon rank-sum test for difference between means was applied to the quantification of 90bp fragments for different conditions (plotted in Supplementary Figure 2). The resulting p-values, corrected for multiple testing using the Bonferroni method, are summarised below:

```
         UMFIX vs SF    NBF vs SF NBF vs UMFIX
Biopsy    0.02791461 6.539409e-05 7.599508e-05
Surgery   0.08424366 6.539409e-05 8.244320e-06
```

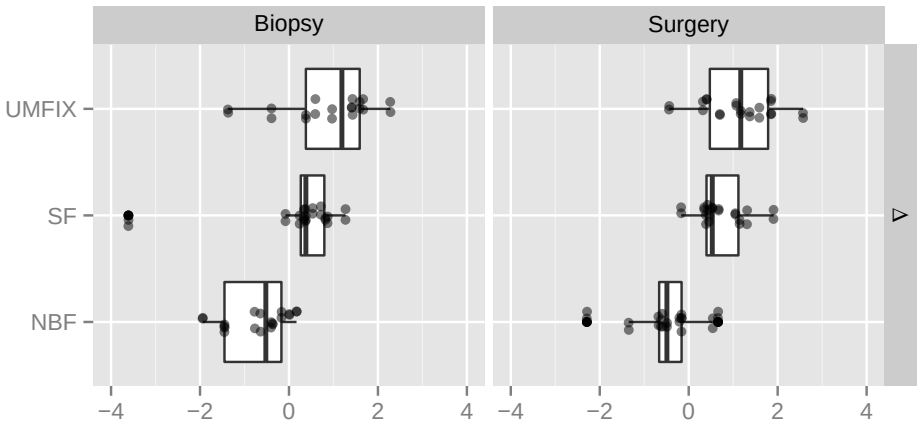

Supplementary Figure 2: Observed $-\Delta Cq$ (Figure 2a from paper): The boxplots show results of PCR assays for DNA size after extraction from snap frozen (SF), buffered formalin (NBF) and methanol (UMFIX) fixation from matched biopsy and surgical samples from 11 HGSOC patients. Negative ΔCq values are shown for convenience.

5.2 qPCR of 41bp, 129bp and 305bp fragments using KAPA hgDNA Quantification and QC Kit (KAPA Biosystems)

Q-ratios (Q305/Q41 and Q129/Q41) were calculated for each sample after analysis with KAPA hgDNA Quantification and QC Kit and are summarised in Supplementary Figure 3.
Statistical test: The Wilcoxon rank-sum test for difference between means was applied to the quantification of Q-ratios for different conditions (plotted in Supplementary Figure 3). The resulting p-values, corrected for multiple testing using the Bonferroni method, are summarised below:

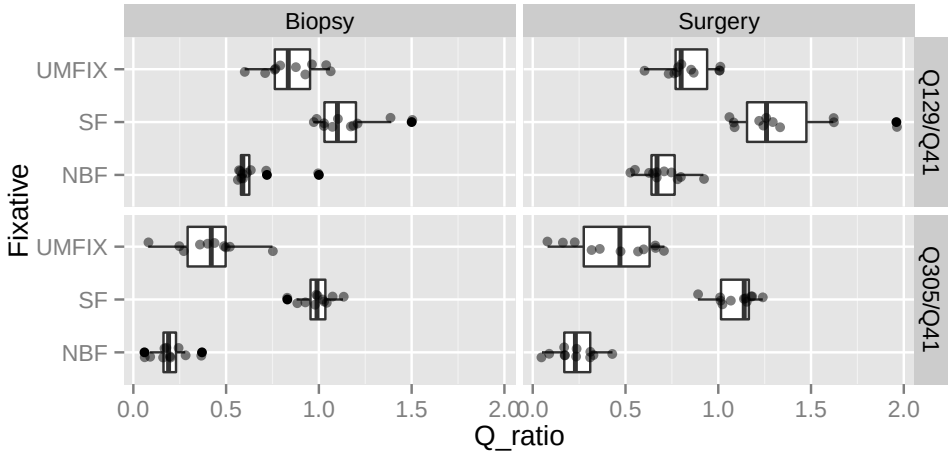

Supplementary Figure 3: Observed Q-ratios (Figure 2b from paper). The boxplots show results of PCR assays for DNA size after extraction from snap frozen (SF), buffered formalin (NBF) and methanol (UMFIX) fixation from matched biopsy and surgical samples from 11 HGSOC patients.

	UMFIX vs SF	NBF vs SF	NBF vs UMFIX
Q305/Q41.Biopsy	0.0009831970	0.0009831970	0.02178779
Q305/Q41.Surgery	0.0009424107	0.0009424107	0.03880384
Q129/Q41.Biopsy	0.0052738487	0.0012908224	0.01822342
Q129/Q41.Surgery	0.0009424107	0.0009424107	0.03880384

6 Shallow Whole Genome sequencing (sWGS)

DNA from each sample (100ng) was sheared on Covaris S220 (Covaris): duty cycle - 10%, intensity - 5.0, bursts per sec - 200, duration - 300 sec, mode - frequency sweeping, power - 23V, temperature - $5.5\,^{\circ}$C to $6\,^{\circ}$C, water level - 13. Libraries were prepared with the TruSeq Nano DNA LT Sample Prep Kit (Illumina) using a modified protocol - Sample Purification Beads were replaced by Agencourt AMPure XP beads (Beckman Coultier) and size selection after the End Repair was done to remove only the short fragments. Quality and quantity for contructed libraries were assessed with DNA 7500 kit on Agilent 2100 Bioanalyzer and with Kapa Quantification kit (KAPA Biosystems) on 7900HT Fast Real-Time PCR System (Applied Biosystems) according to the supplier's recommendations, respectively. Libraries from 18 barcoded samples were pooled together in equimolar amounts and each pool was loaded on a single lane of a HiSeq Single End Flowcell (Illumina), followed by cluster generation on a cBot (Illumina) and sequencing on a HiSeq 2500 (Illumina) in a single-read 50bp mode.

6.1 Read alignment and copy-number calling

Reads were aligned using bwa-mem v0.7.12-r1039 [10] to the 1000 genomes version of human genome build GRCh37. Picard (http://picard.sourceforge.net) was used to remove duplicate reads.
In order to perform legitimate comparisons between samples for copy-number calling, all samples must have approximately the same read coverage. Therefore, for each sample triplet (UMFIX, SF or NBF), reads were downsampled to the condition with the lowest number reads to account for any variation in

sequencing depth. QDNAseq [15] was used to filter reads then segment the genome and identify regions of copy-number change (see script copy_number_calling.R in the repository for details).

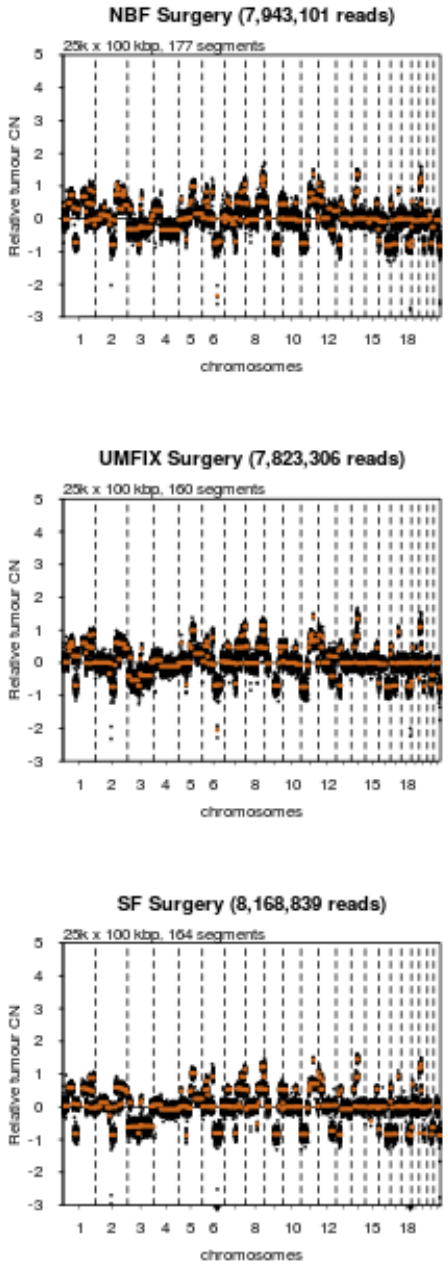

Supplementary Figure 4: Copy-number profiles for patient P2

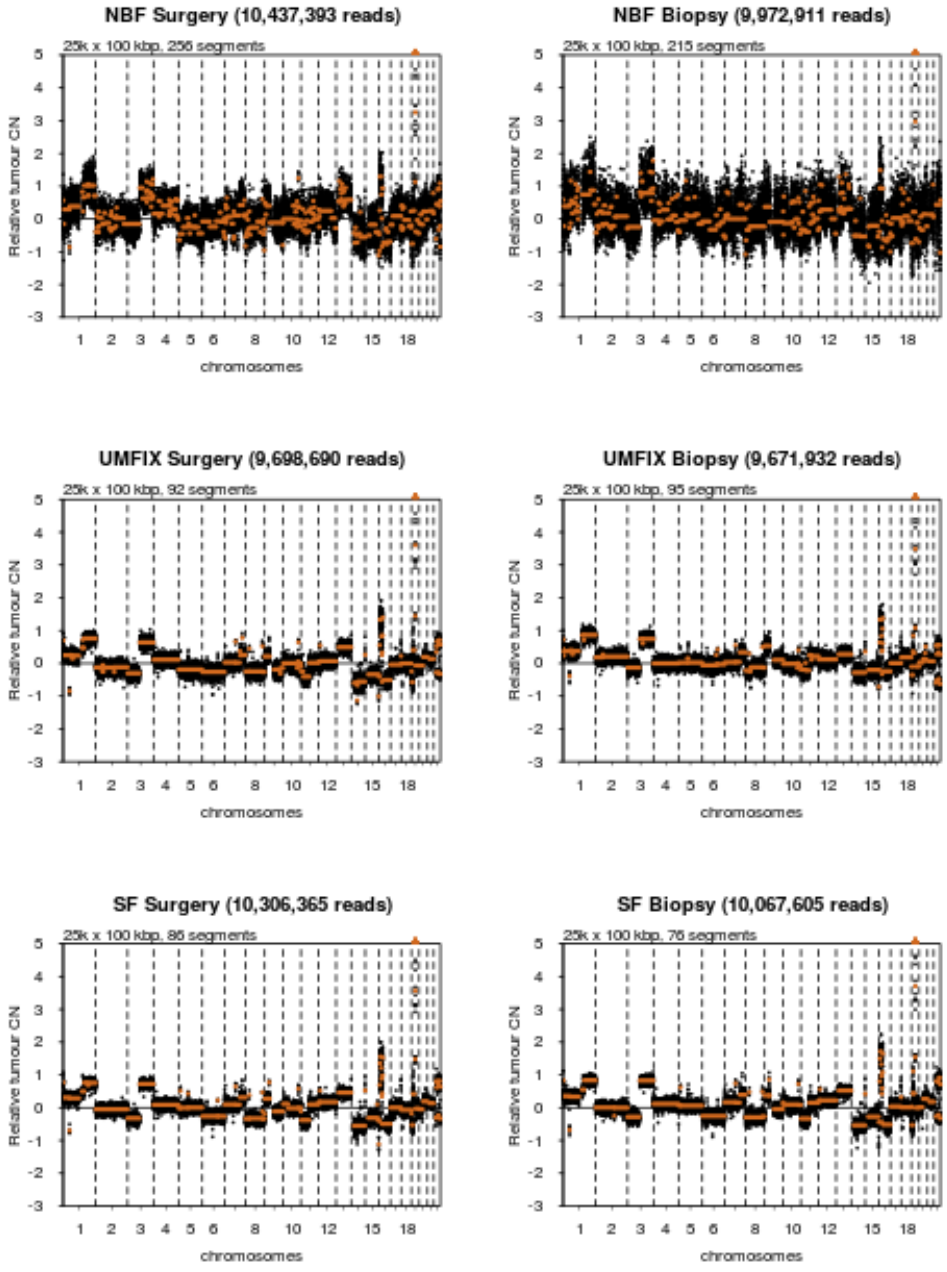

Supplementary Figure 5: Copy-number profiles for patient P3

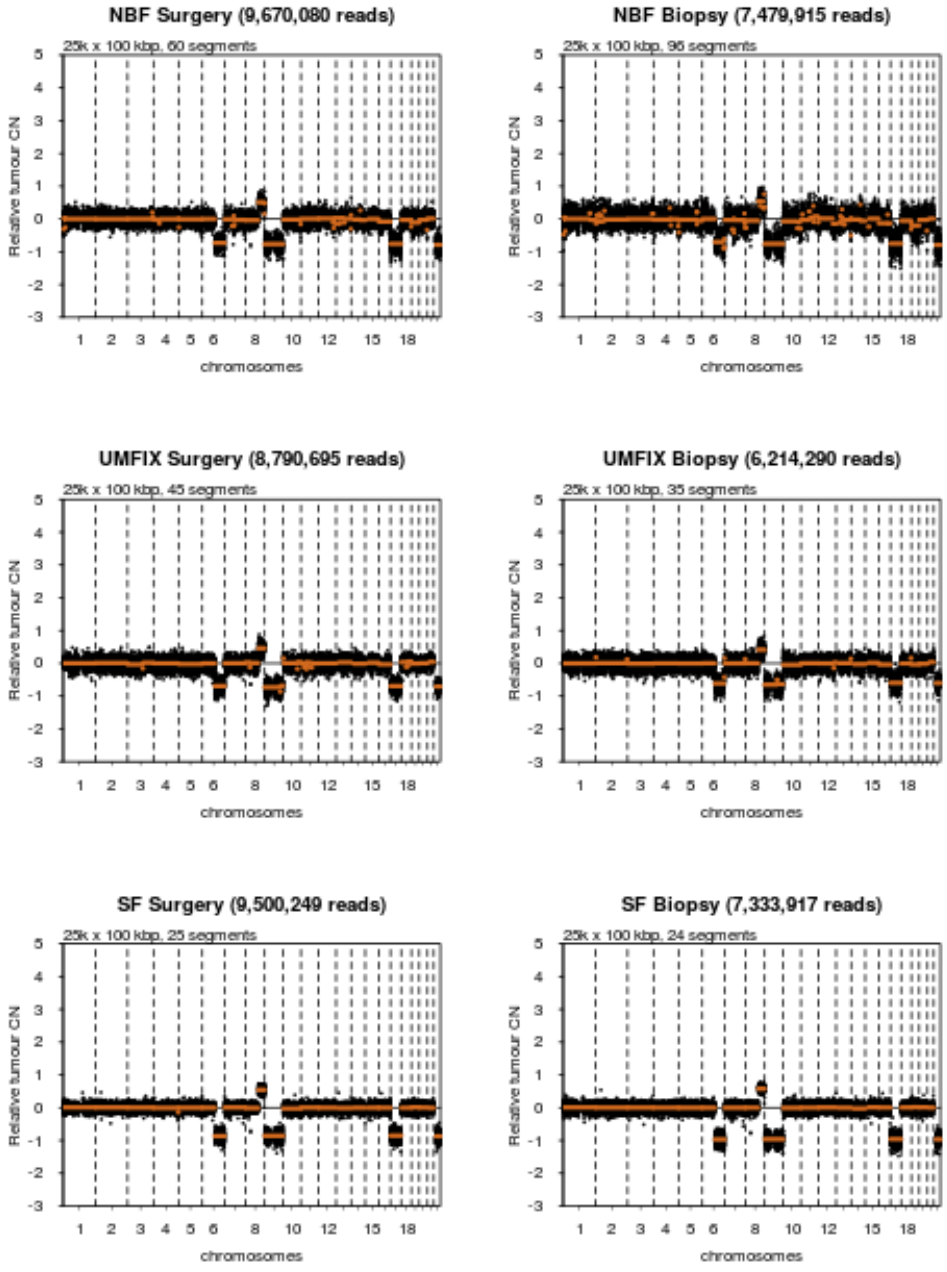

Supplementary Figure 6: Copy-number profiles for patient P4

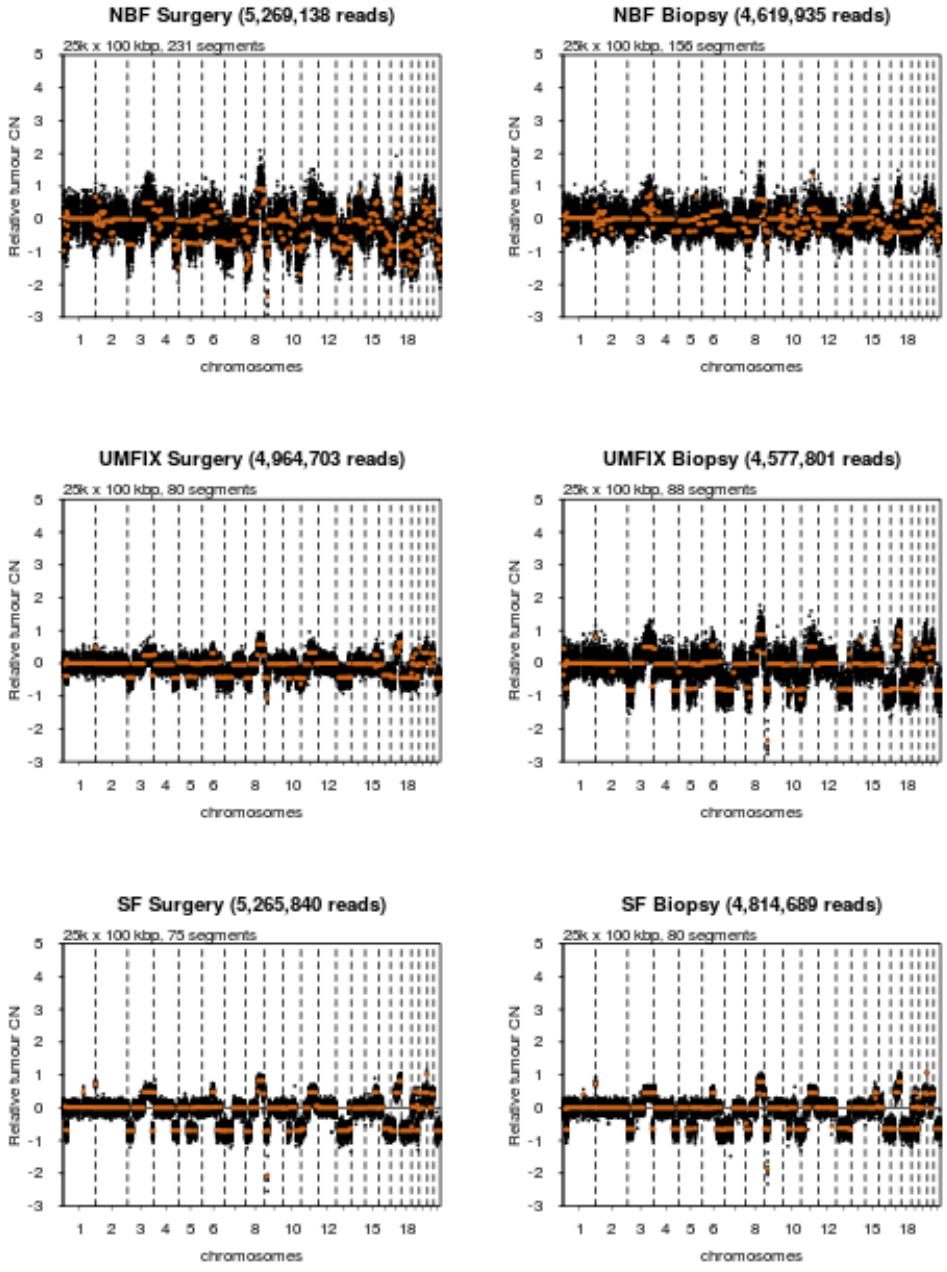

Supplementary Figure 7: Copy-number profiles for patient P5

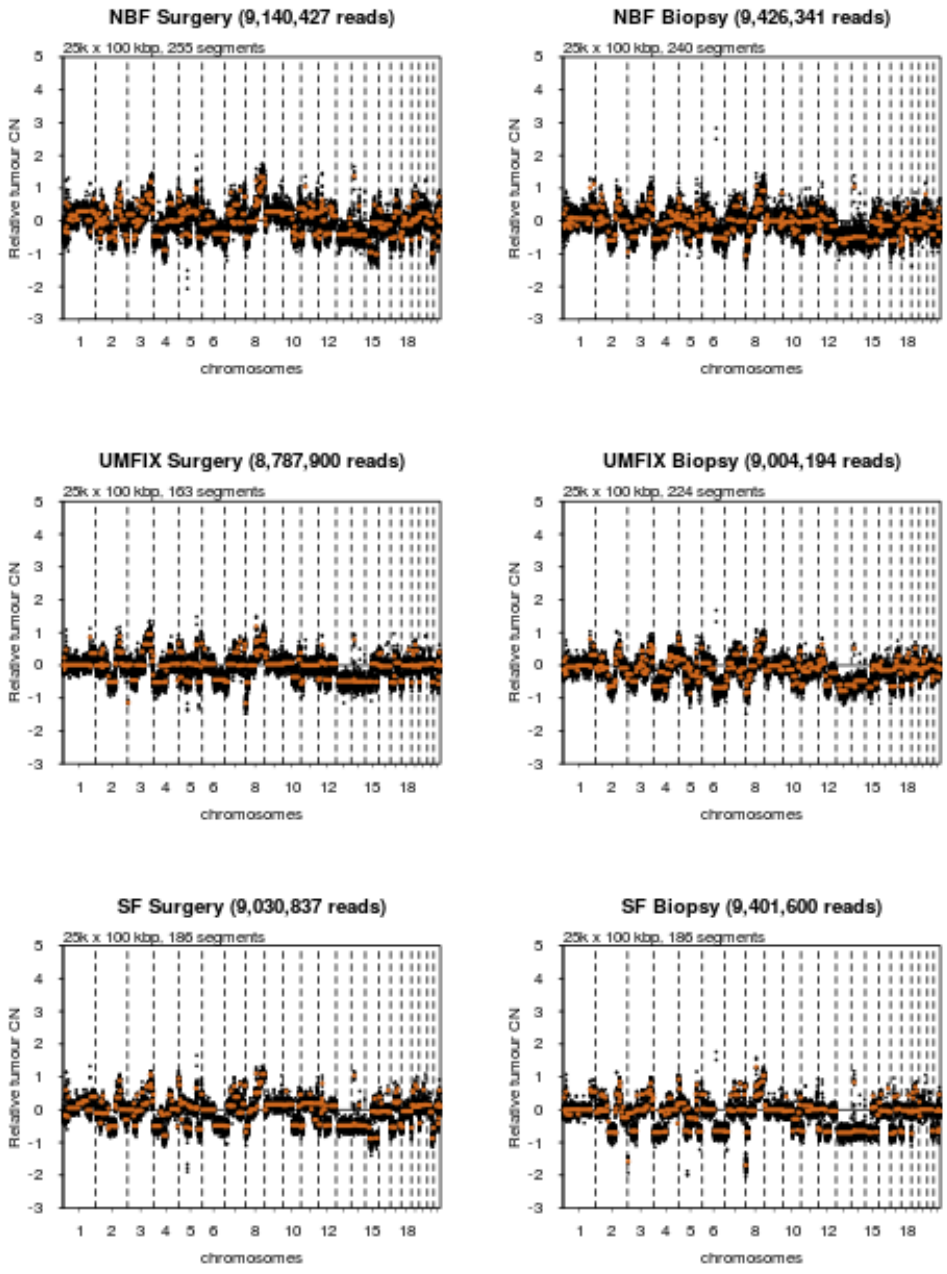

Supplementary Figure 8: Copy-number profiles for patient P6

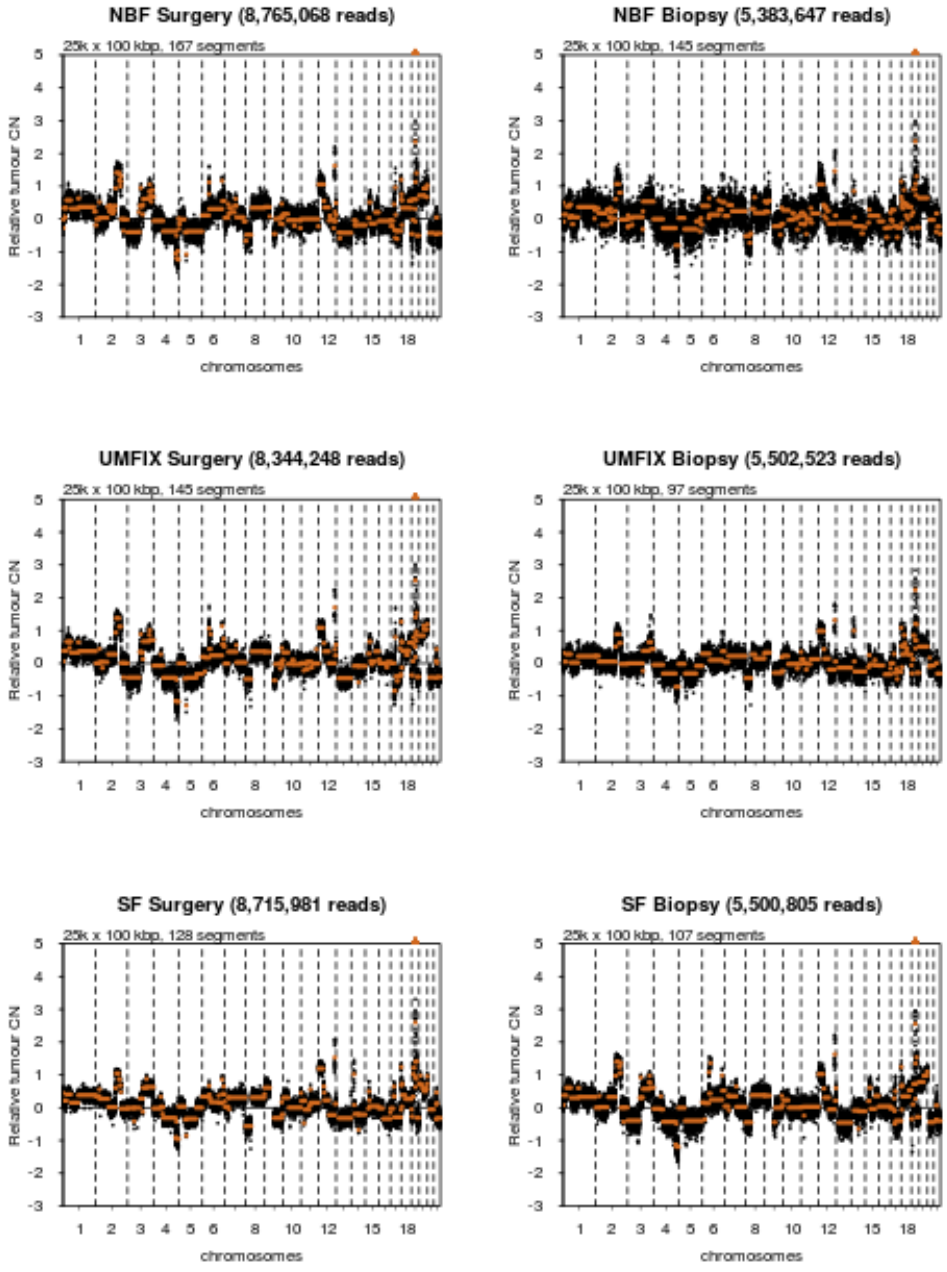

Supplementary Figure 9: Copy-number profiles for patient P8

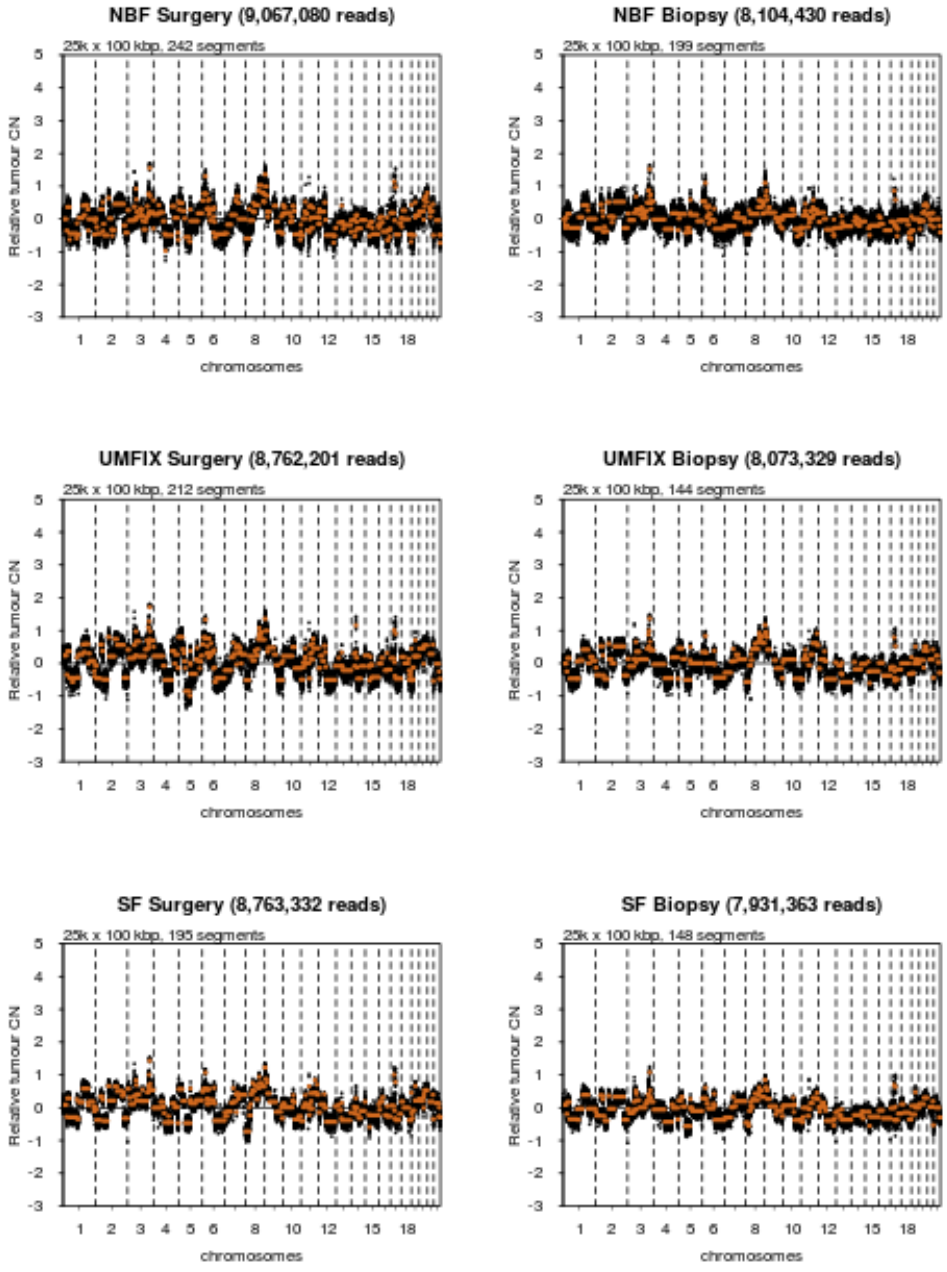

Supplementary Figure 10: Copy-number profiles for patient P9

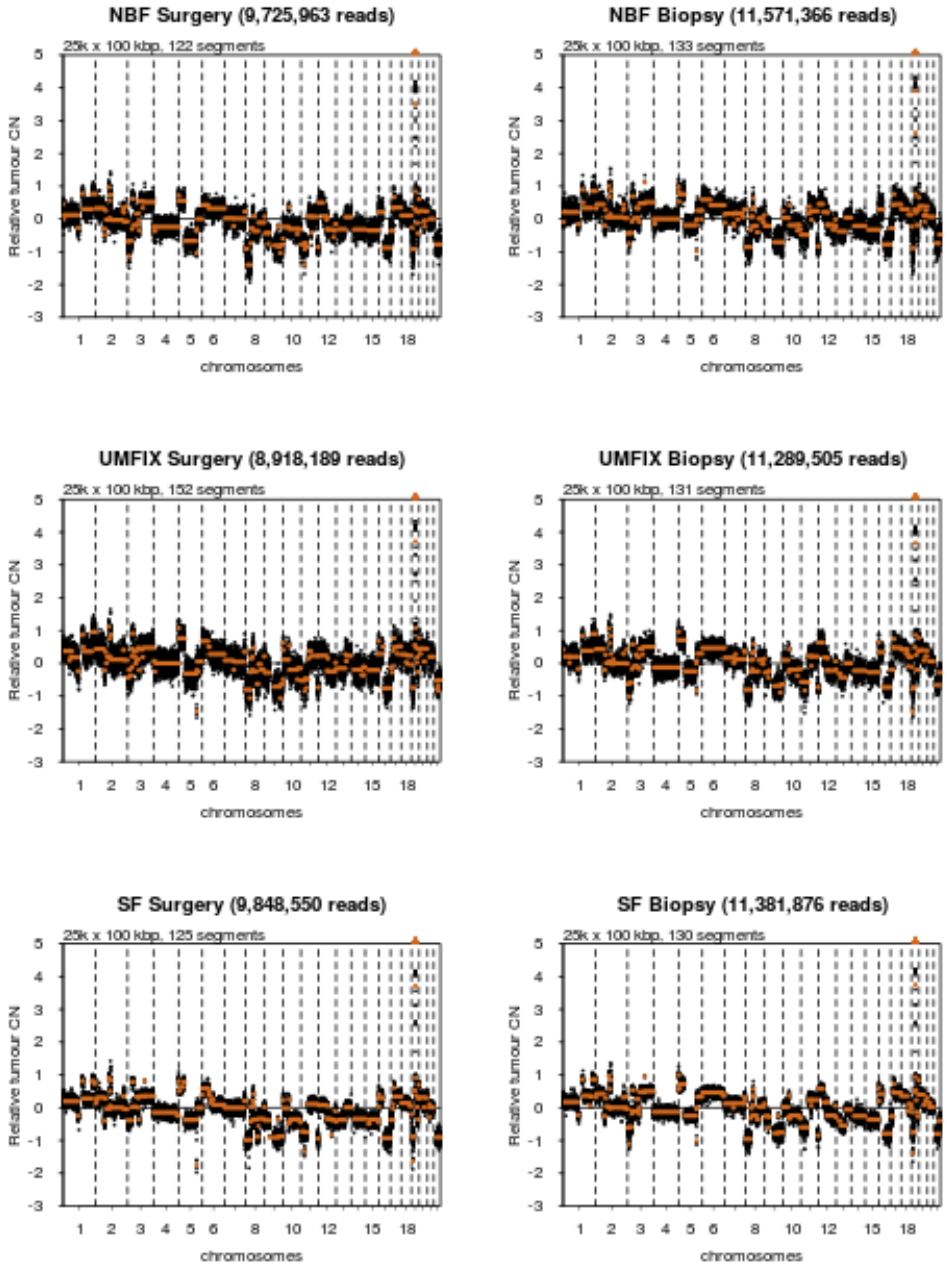

Supplementary Figure 11: Copy-number profiles for patient P11

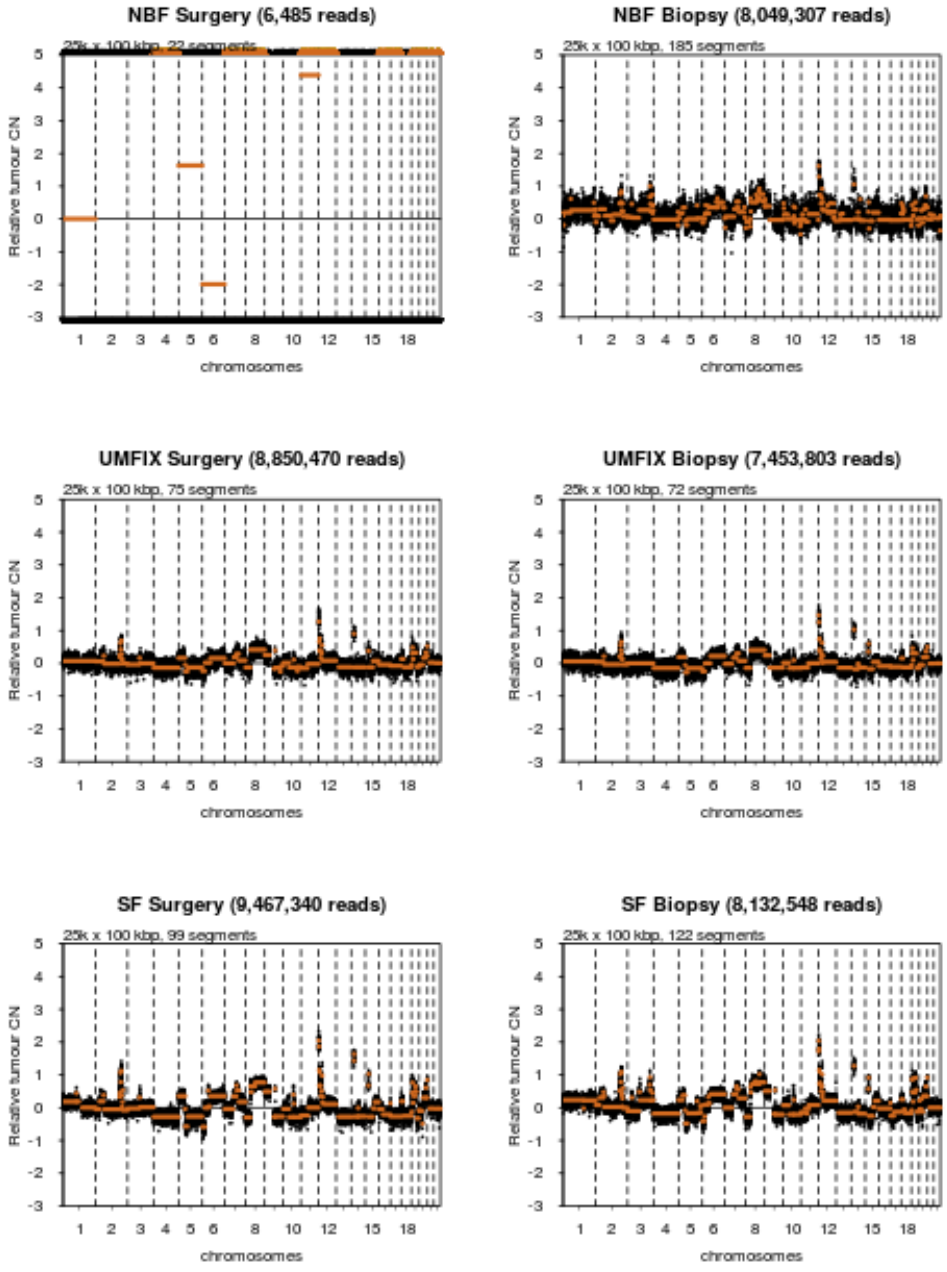

Supplementary Figure 12: Copy-number profiles for patient P13

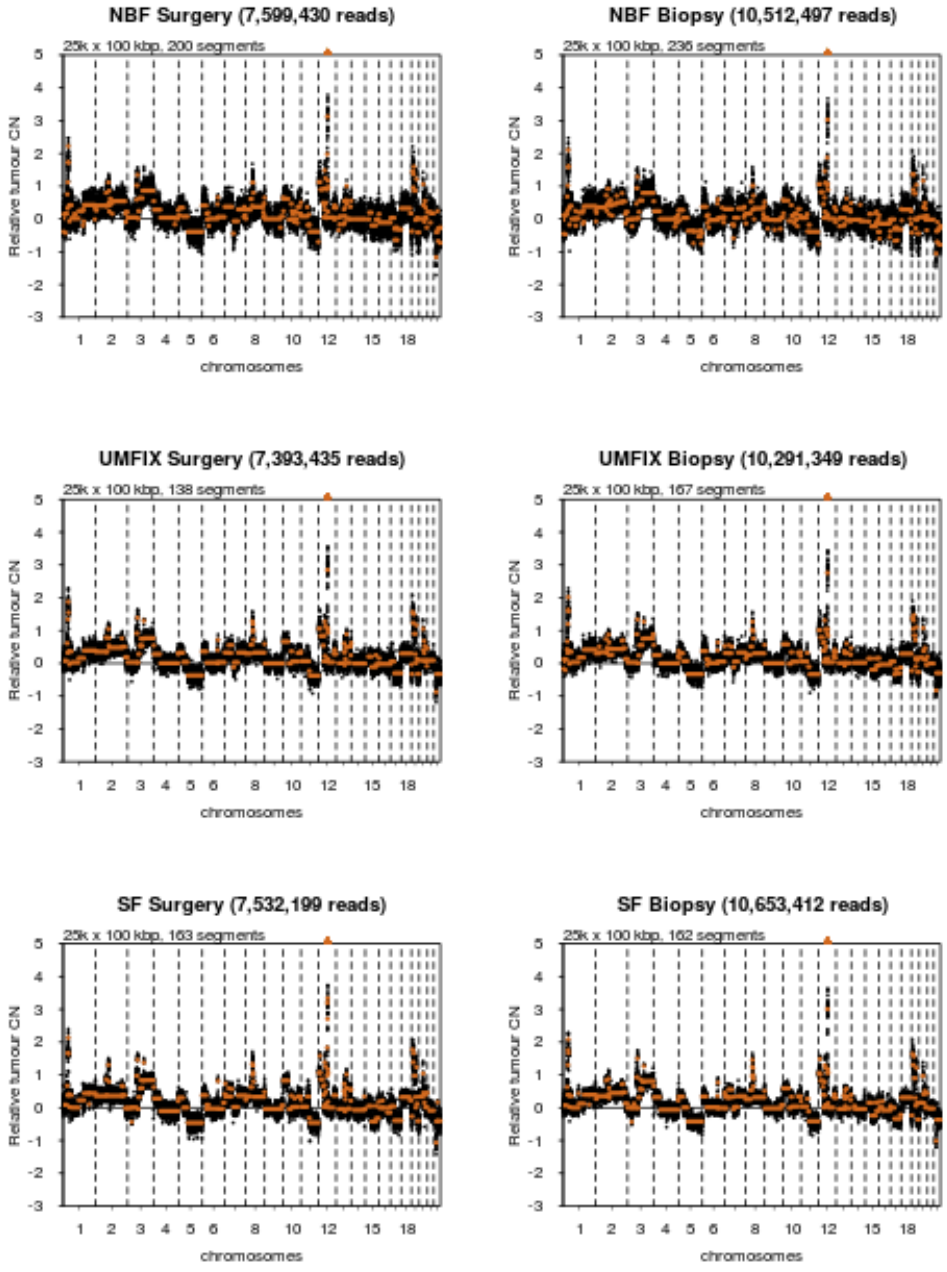

Supplementary Figure 13: Copy-number profiles for patient P14

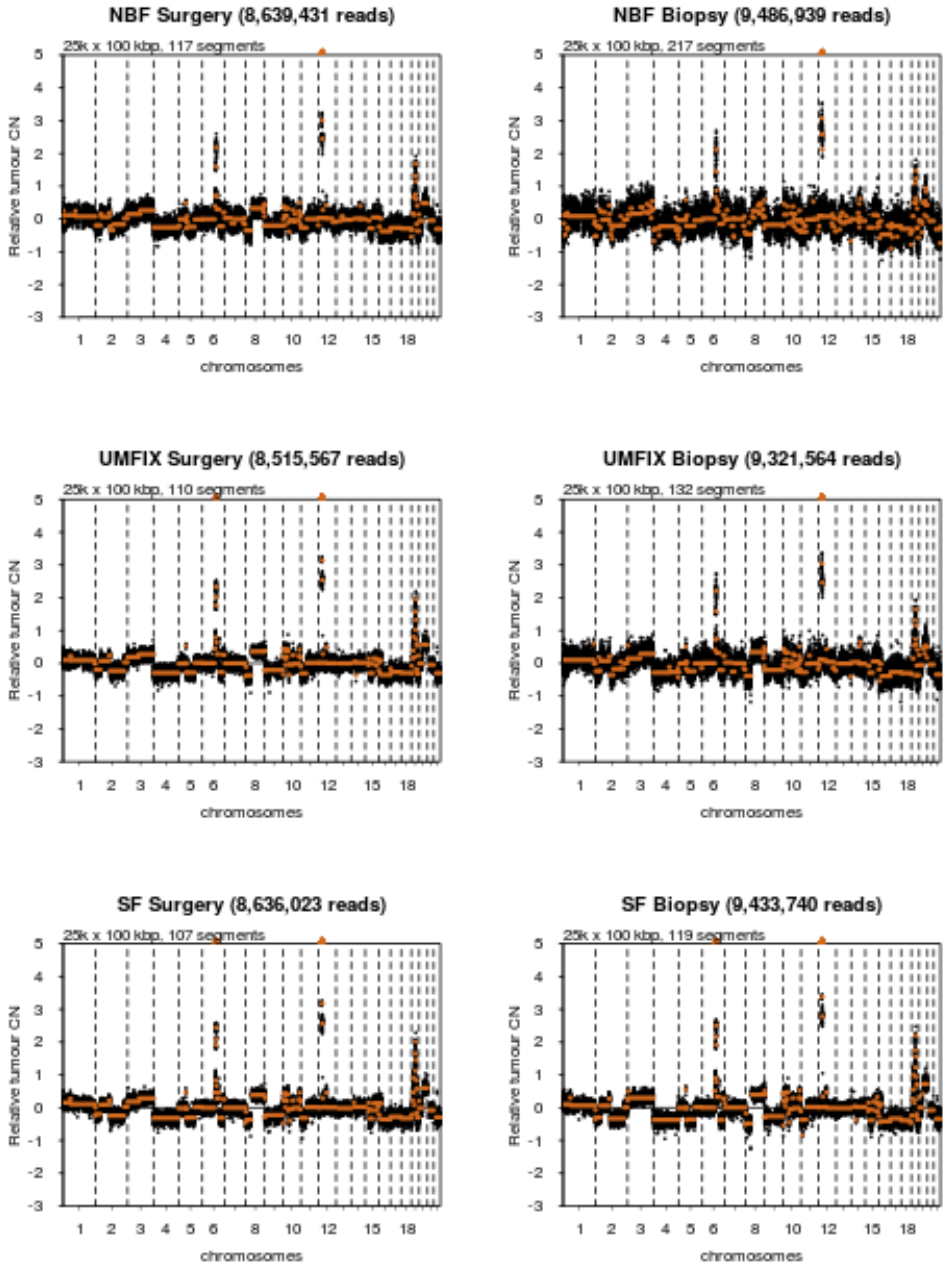

Supplementary Figure 14: Copy-number profiles for patient P15

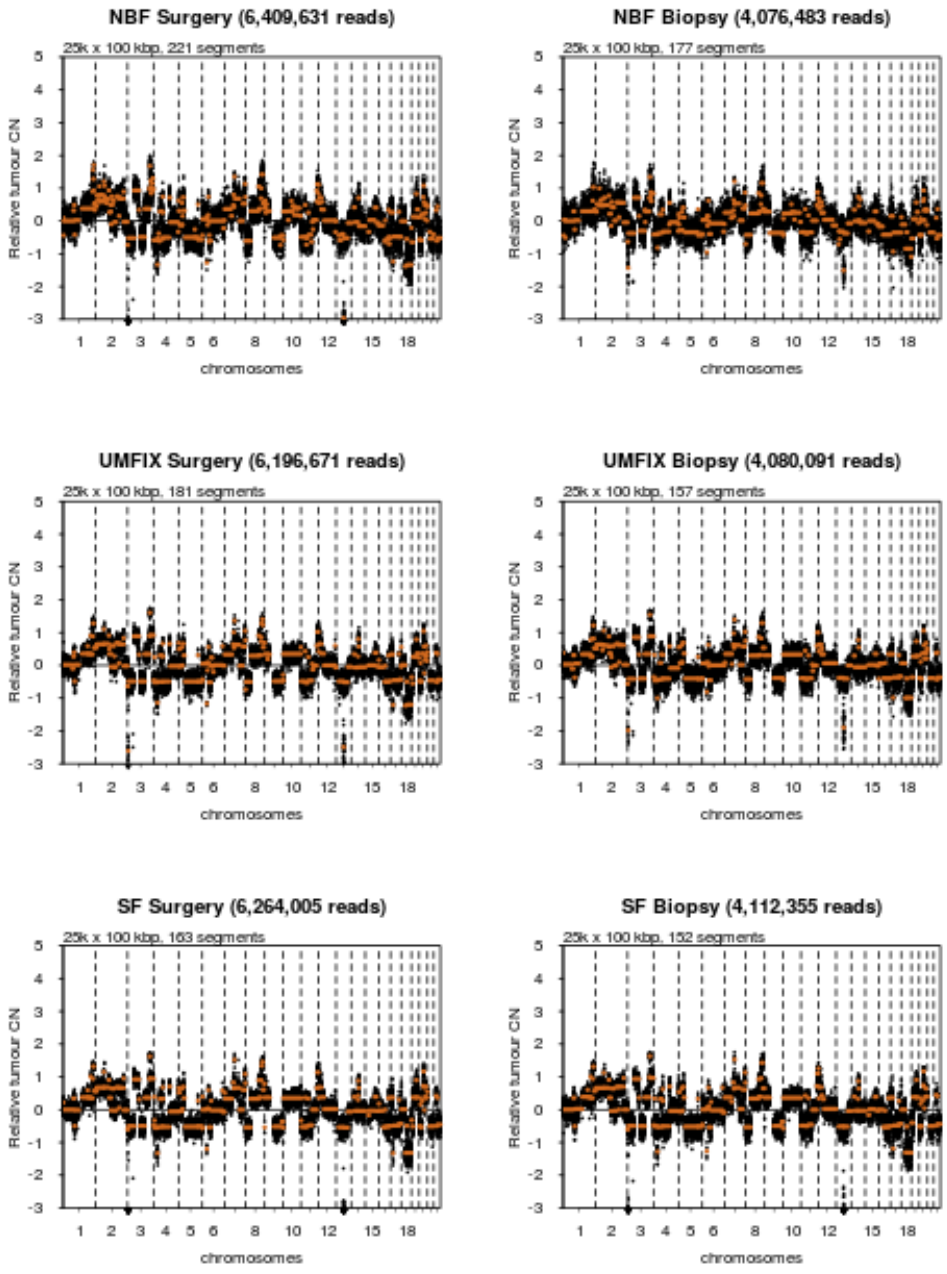

Supplementary Figure 15: Copy-number profiles for patient P16

6.2 Genome-wide comparison of copy-number calling

Although care was taken to sample tumour material as uniformly as possible for each of the three conditions (UMFIX, NBF and SF), there was naturally some variability in the tumour content of each sample. When generating relative median normalised copy-number profiles, this variation in tumour content manifests as variable deviations from 0 for the same copy-number across conditions. To account for this source of variation, Spearman rank correlation was used as a metric to compare copy-number profiles

as it uses a categorical deviation (e.g. higher or lower) rather than the relative copy-number estimates directly. Another factor confounding comparison was that each sample had a different genome segmentation, making direct comparison of copy-number impossible. Correlation was therefore calculated on a union of all segments identified across conditions to account for differences in the segment numbers. Results are summarised in Supplementary Figure 16.

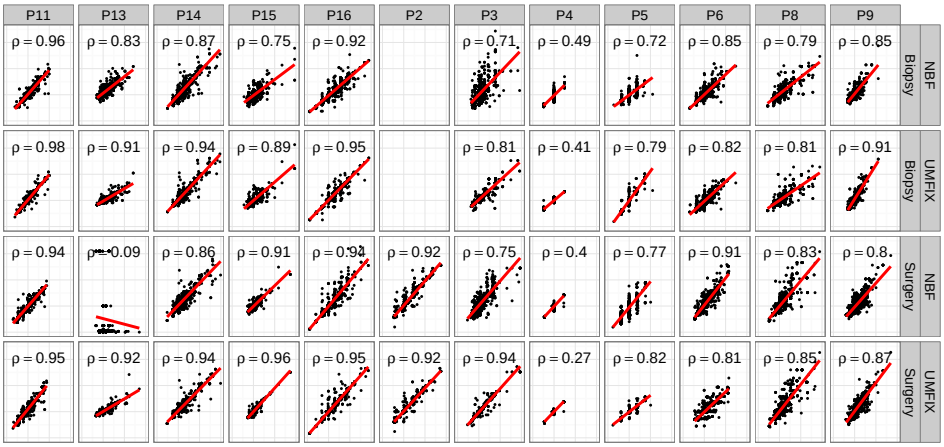

Supplementary Figure 16: Comparison of copy-number values (Figure 2c from paper). Scatter plots show correlation between median normalised copy-number profiles from shallow WGS of SF compared to NBF or UMFIX biopsy and surgical samples from 12 patients. Spearman's rank correlation rho is shown.

6.3 Comparison of copy-number segment variation.

To look at the accuracy of the copy-number estimate of each segment, we observed the distribution of read depth variance across all segments for samples in UMFIX, NBF or SF. Those with a higher variance are expected to have a higher chance of giving an incorrect copy-number estimate. A summary of the variance observed across 30,104 segments can be found in Supplementary Figure 17.

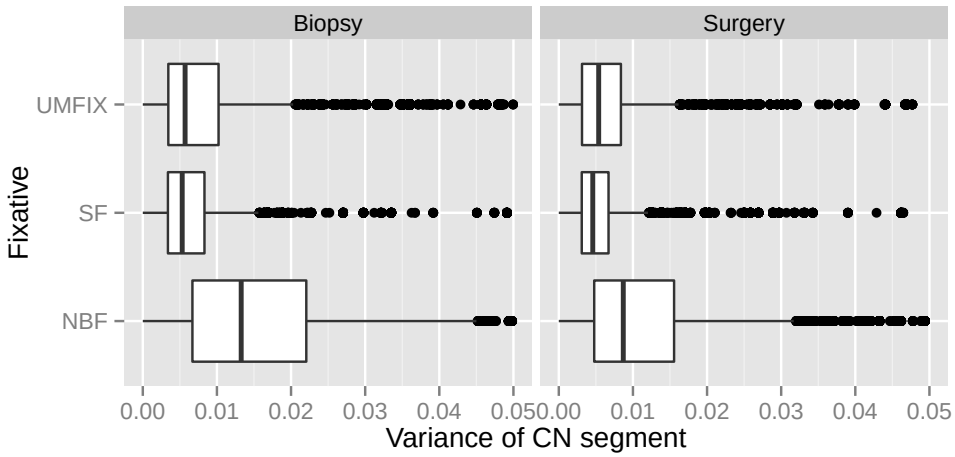

Supplementary Figure 17: Comparison of copy-number variance (Figure 2d from paper). Boxplots show observed variance for each copy-number segment (n=90,312) in 69 samples from 12 patients.

Statistical test: The Wilcoxon rank-sum test for difference between means was applied to the segment variance for different conditions (plotted in Supplementary Figure 17). The resulting p-values, corrected for multiple testing using the Bonferroni method, are summarised below:

	UMFIX vs SF	NBF vs SF	NBF vs UMFIX
Biopsy	4.598574e-71	0	0
Surgery	5.192374e-40	0	0

7 Tagged-Amplicon Sequencing (TAm-Seq)

Targeted sequencing of 48 amplicons in TP53, PTEN, EGFR, PIK3CA, KRAS and BRAF genes was performed as described previously [7]. All libraries were pooled and quantify using DNA 1000 kit on Agilent 2100 Bioanalyzer and KAPA SYBR® FAST ABI Prism qPCR Kit (KAPA Biosystems) on 7900HT Fast Real-Time PCR System (Applied Biosystems) according to the supplier's recommendations. All samples were analysed in duplicate.

7.1 Read alignment and variant calling

Reads were aligned using bwa-mem v0.7.12-r1039 [10] to the 1000 genomes version of human genome build GRCh37, retaining duplicate reads. HaplotypeCaller as part of the Genome Analysis Tool Kit[3] was used to call variants and the Ensembl variant effect predictor[12] used to annotate variants.

7.2 Manual curation of SNVs and performance assessment

All reported mutations were verified by visual inspection using the Integrated Genomics Viewer software [18] using the following steps:

- bam files for both technical replicates were uploaded into IGV
- bam files for two independent samples from the same sequencing (but from different patients) run were uploaded into IGV

- manual inspection of each variant was performed by visual comparison of all four bam files

Each SNV was labelled as either a true variant (true positive, TP), or artefact (false positive, FP) using the following criteria

- if the SNV was present in one technical replicate but not the other, the SNV was considered "false positive"
- if the SNV was present at low frequency ($< 10\%$) in the independent samples, the SNV was considered "false positive"
- if the SNV was present at high frequency across all samples from the same sequencing run the SNV was considered "false positive"
- if the SNV was present at very low frequency ($< 1\%$), the SNV was considered "false positive"
- if the SNV was present at high frequency, and not present at a similar frequency in the independent samples (but not across all samples form the same sequencing run) SNV was condsidered "true positive"
- if the SNV was present at low frequency but higher than 5% and present at high frequency or not present in the independent samples the SNV was considered "true positive"

The union of all called SNVs in a patient, across all samples was then used to determine if a SNV was not called but should have been (false negative, FN), or if an artefactual variant was not called (true negative, TN). Two measures were then calulated: sensitivity $TP/(TP + FN)$ and specificity $TN/(TN + FP)$. Figure 18 provides a summary of these metrics for each of the fixatives.

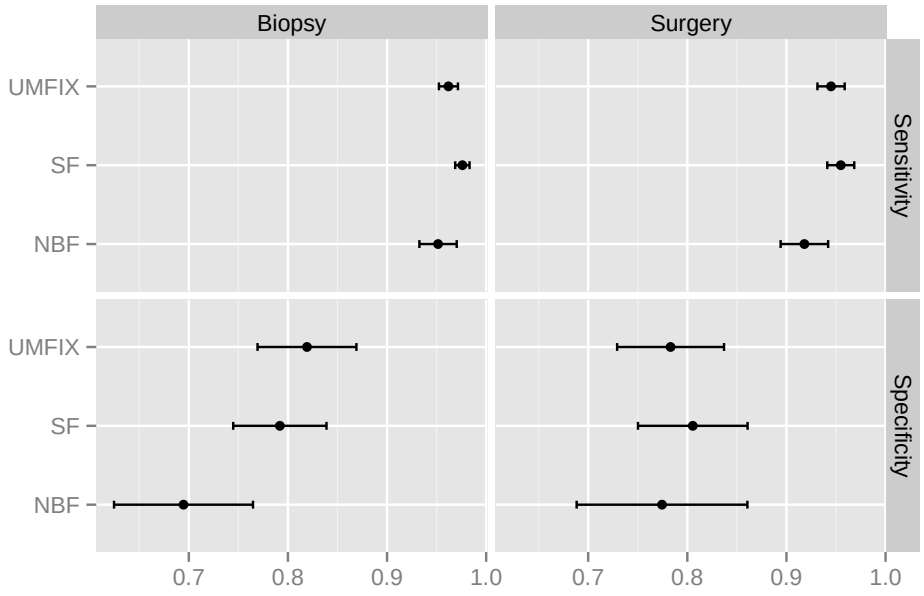

Supplementary Figure 18: Observed SNV sensitivity and specificity (Figure 3c from paper). Sensitivity (top) and specificity (bottom) for manually curated SNV calls (n=546) from TAm-SEQ of biopsy and surgical samples from 11 patients. Bars indicate the 95% confidence interval around the indicted mean.

7.3 Mutation signature analysis

All non-reference bases appearing in sWGS data were identified using samtools mpileup[11]. Non-reference bases in TAm-Seq data were identified using the h5vc package in Bioconductor[13]. Together these base changes are presumed to be made up of a combination of sequencing artefacts, fixation artefacts, germ-line SNPs, and somatic SNVs. These changes were filtered for putative germline SNPs using dbsnp138, leaving only artefactual changes and true somatic changes (total = 255,376 base changes, see script signature_preprocess.R for details). These base changes were further grouped into four categories: COMMON, those changes found across all conditions (UMFIX, NBF and SF) in a patient; NBF, changes only found in NBF fixed samples; SF, changes only found in SF samples; UMFIX, changes only found in UMFIX samples.

The trinucleotide context of these changes (the bases immediately flanking the change) were extracted from the reference genome and subsequently analysed using the SomaticSignature package in Bioconductor[8]. The SomaticSignature package implements a method, which has been previously applied to identify mutational signatures[1]. These mutational signatures are distinct trinucleotide patterns which may represent a particular mutational force acting on the DNA, such as APOBEC cytosine deamination which occurs in the context of TCW, T and W represent nucleotide abiguity codes[14]. While this technique has been applied to collections of somatic mutations to attempt to understand the underlying mutational mechanisms operational in the tumour, here we use the same idea to model all base changes, predominantly made up of noise, to understand what might be causing this sequencing noise.

Briefly, the observed base changes were summarised by a $C \times S$ frequency matrix which contained the observed frequency of each trinucleotide, for each base change S (96 possible combinations), for each category C, (COMMON, NBF, SF, and UMFIX). Non-negative matrix factorisation (NMF) was then applied to this matrix, which decomposed the matrix into two components representing distinct mutational signatures (visually represented in Supplementary Figure 20) and the contribution of each signature to each condition (visually represented in Supplementary Figure 21).

Initally, an assesment had to be made as to how many signatures there were present in the collection of observed base changes. To determine this, NMF was run with 2, 3, and 4 signatures specified and the variance explained by these signatures was observed (Supplementary Figure 19). 3 signatures explained 100% of the variance and as such analysis was run with 3 signatures.

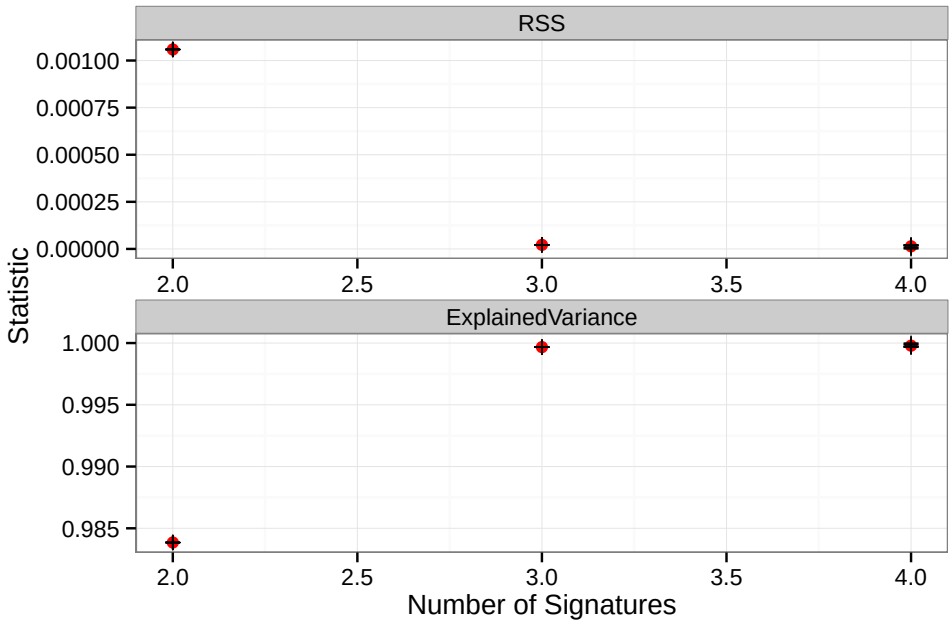

Supplementary Figure 19: Number of mutation signatures versus residuals sum of squares (top) and explained variance (bottom).

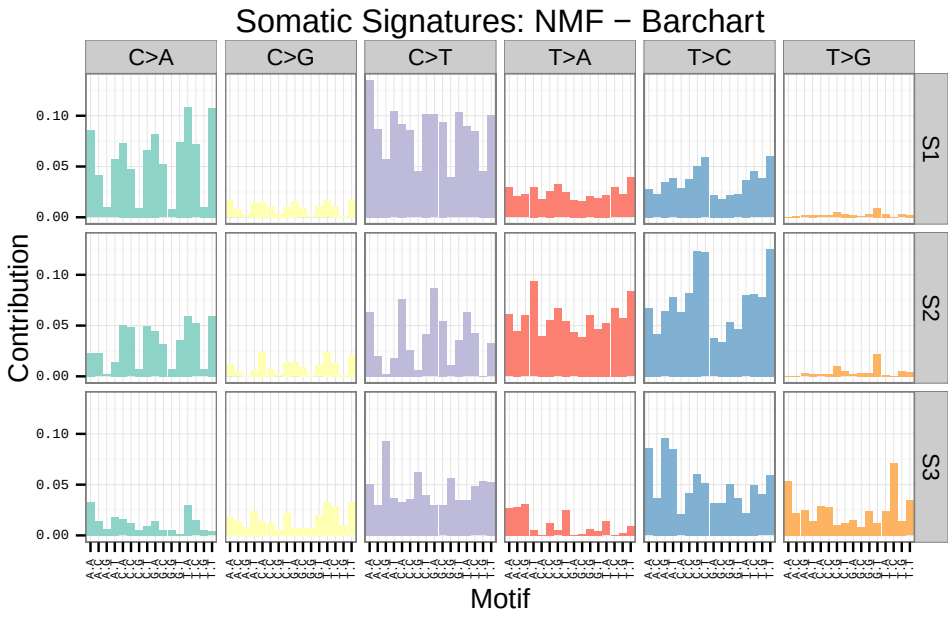

Supplementary Figure 20: Mutation signatures (Figure 3a from paper): Bar plots of the 3 somatic mutation signatures (S1-S3) identified by non-negative matrix factorisation using all non-reference bases observed in sWGS and TAm-SEQ sequencing data in 69 samples from 12 patients (n=255,376). Bar plots are grouped by the observed base change with individual bars showing the proportion observed at different tri-nucleotide sequences.

Supplementary Table 5: Summary of comparisons between UMFIX and NBF: This table provides an overview of the differences and similarities between UMFIX and NBF along with supporting references.

Feature	NBF	UMFIX	Evidence
DNA, RNA, protein preservation	poor	good	[9, 2, 6, 17, 20]
Changes to DNA, RNA, protein structure	yes	no	[9, 17, 20]
DNA amplifiable fragments (>400bp)	no/few	yes/many	[17, 19, 20, 22]
DNA molecular weight after fixative exposure (>72hrs)	decreased	unchanged	[19, 20, 22]
Artificial DNA mutations	reported	not reported	[21, 16, 4]
H&E	good	good	[9, 19, 20]
IHC	good	good	[9, 20]

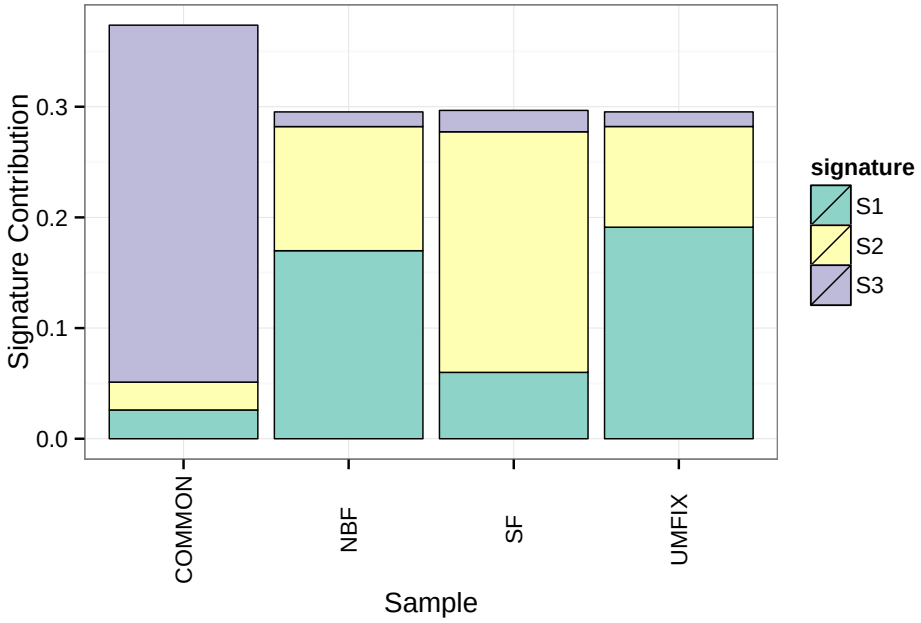

Supplementary Figure 21: Contribution of mutation signature (Figure 3b from paper): Stacked bar plots show the proportion of the 3 mutation signatures observed only in SF and NBF or UMFIX fixed samples compared to signatures present in all samples from an individual patient (common)

8 Comparison with previous literature

To identify previous studies comparing the performance of UMFIX and NBF for fixation of cancer samples PubMed and Google were used with the following search terms: "fixative and sequencing", "fixative and NGS", "UMFIX", "FFPE and NGS", "UMFIX and sequencing". Key observations made in papers found during this search can be found in Supplementary Table 5. For excellent reviews in the area see [9, 4, 5]

9 Instructions for reproducing analysis

In order to compile the supplementary material you will need to undertake the following steps:

- clone the paper repository https:/bitbucket.org/britroc/fixation
- install R (we recommend using RStudio)
- install latex
- install the following R/Bioconductor packages: ggplot2, reshape2, plyr, xlsx, QDNAseq and SomaticSignatures
- compile the sweave document supplementary_material.Rnw

In order to reconstruct the full analysis, bam files and content files should be downloaded from the European Genome Archive, accession EGAS00001001433, and the following scripts modified to point to the directory containing the bam files before running:

- sWGS_downsample.R
- copy_number_calling.R
- base_change_calling.R
- signature_preprocess.R

Supplementary Table 6: Histoscores, tumour cellularity and TP53 mutant allele frequency. * - sample stained, but not analysed (missing paired sample), AF = allele frequency

Patient ID	Fixation	Tissue type	p53	CK7	Pax8	WT1	CK20	Cellularity (%)	TP53 mut AF
P1	NBF	Ctrl	10	2	12	112	0	<10	NA
P1	NBF	Tu	4	16	14	18	3	70	NA
P1	UMFIX	Ctrl	0	0	48	34	13	<10	NA
P1	UMFIX	Tu	10	128	97	38	7	90	NA
P2	NBF	Ctrl	0	4	14	141	6	<10	NA
P2	NBF	Tu	191	98	145	201	0	70	NA
P2	UMFIX	Ctrl	64	4	61	85	0	<10	NA
P2	UMFIX	Tu	168	30	103	99	3	70	NA
P3	NBF	Bx	4	105	77	101	5	80	0.781
P3	NBF	Ctrl	2	6	9	16	21	<10	NA
P3	NBF	Tu	54	124	160	201	3	80	0.872
P3	SF	Bx	NA	NA	NA	NA	NA	NA	0.805
P3	SF	Tu	NA	NA	NA	NA	NA	NA	0.779
P3	UMFIX	Bx	0	108	134	48	1	70	0.731
P3	UMFIX	Ctrl	0	12	82	12	15	<10	NA
P3	UMFIX	Tu	8	136	150	166	5	85	0.805
P4	NBF	Bx	107	98	151	161	NA	40	0.697
P4	NBF	Ctrl	4	0	29	112	NA	<10	NA
P4	NBF	Tu	132	169	205	200	NA	40	0.699
P4	SF	Bx	NA	NA	NA	NA	NA	NA	0.936
P4	SF	Tu	NA	NA	NA	NA	NA	NA	0.812
P4	UMFIX	Bx	88	104	154	47	NA	30	0.539
P4	UMFIX	Ctrl	0	0	73	53	NA	<10	NA
P4	UMFIX	Tu	155	147	167	140	NA	35	0.661
P5	NBF	Bx	148	10	130	5	3	95	0.194
P5	NBF	Ctrl	6	13	39	37	12	<10	NA
P5	NBF	Tu	179	22	142	168	0	70	0.604
P5	SF	Bx	NA	NA	NA	NA	NA	NA	0.528
P5	SF	Tu	NA	NA	NA	NA	NA	NA	0.606
P5	UMFIX	Bx	163	6	104	100	3	90	0.631
P5	UMFIX	Ctrl	2	16	41	12	1	<10	NA
P5	UMFIX	Tu	84	0	67	68	0	70	0.261
P6	NBF	Bx	152	63	NA	47	3	80	0.535
P6	NBF	Ctrl	0	0	7	65	0	<10	NA
P6	NBF	Tu	168	100	93	203	1	95	0.624
P6	SF	Bx	NA	NA	NA	NA	NA	NA	0.631
P6	SF	Tu	NA	NA	NA	NA	NA	NA	0.620
P6	UMFIX	Bx	151	50	161*	108	12	95	0.604
P6	UMFIX	Ctrl	0	0	54	96	0	<10	NA
P6	UMFIX	Tu	132	76	103	176	0	95	0.489
P7	NBF	Ctrl	2	0	11	12	20	<10	NA
P7	NBF	Tu	60	124	153	175	36	85	NA
P7	UMFIX	Ctrl	0	0	25	11	38	<10	NA
P7	UMFIX	Tu	32	110	123	103	3	80	NA
P8	NBF	Bx	117*	73	107	109	NA	70	0.737
P8	NBF	Ctrl	6	0	10	100	NA	<10	NA
P8	NBF	Tu	183	142	156	41	NA	70	0.850
P8	SF	Bx	NA	NA	NA	NA	NA	NA	0.853

P8	SF	Tu	NA	NA	NA	NA	NA	NA	0.773
P8	UMFIX	Bx	NA	59	146	32	NA	65	0.675
P8	UMFIX	Ctrl	2	4	105	72	NA	<10	NA
P8	UMFIX	Tu	195	145	166	69	NA	90	0.863
P9	NBF	Bx	131	82	100	45	12	NA	NA
P9	NBF	Bx	46	10	32	49	0	45	0.446
P9	NBF	Ctrl	2	2	18	8	3	<10	NA
P9	NBF	Tu	170	105	165	0	2	95	0.777
P9	SF	Bx	NA	NA	NA	NA	NA	NA	0.551
P9	SF	Tu	NA	NA	NA	NA	NA	NA	0.682
P9	UMFIX	Bx	61	26	81	28	0	NA	NA
P9	UMFIX	Bx	56	31	113	65	0	60	0.653
P9	UMFIX	Ctrl	4	2	35	0	6	<10	NA
P9	UMFIX	Tu	168	84	117	168	35	90	0.821
P10	NBF	Ctrl	6	0	19	95	0	<10	NA
P10	NBF	Tu	94	75	106	76	7	60	NA
P10	UMFIX	Ctrl	68	6	52	72	3	<10	NA
P10	UMFIX	Tu	19	12	86	24	7	50	NA
P11	NBF	Bx	183	128	55	75	6	70	0.848
P11	NBF	Ctrl	16	32	32	70	117	<10	NA
P11	NBF	Tu	183	128	88	185	3	65	0.880
P11	SF	Bx	NA	NA	NA	NA	NA	NA	0.922
P11	SF	Tu	NA	NA	NA	NA	NA	NA	0.930
P11	UMFIX	Bx	156	138	88	40	5	70	0.846
P11	UMFIX	Ctrl	10	17	62	17	31	<10	NA
P11	UMFIX	Tu	161	106	93	60	2	70	0.867
P12	NBF	Bx	NA	NA	NA	NA	NA	30	0.413
P12	NBF	Tu	NA	NA	NA	NA	NA	30	0.333
P12	SF	Bx	NA	NA	NA	NA	NA	NA	0.439
P12	SF	Tu	NA	NA	NA	NA	NA	NA	0.659
P12	UMFIX	Bx	NA	NA	NA	NA	NA	30	0.480
P12	UMFIX	Tu	NA	NA	NA	NA	NA	27	0.360
P13	NBF	Bx	22	25	169	56	8	NA	0.236
P13	NBF	Ctrl	8	25	65	109	2	<10	NA
P13	NBF	Tu	16	37	146	59	9	NA	0.541
P13	SF	Bx	NA	NA	NA	NA	NA	NA	0.393
P13	SF	Tu	NA	NA	NA	NA	NA	NA	0.321
P13	UMFIX	Bx	0	74	122	3	1	NA	0.224
P13	UMFIX	Ctrl	28	20	97	57	3	<10	NA
P13	UMFIX	Tu	16	20	112	28	16	NA	0.192
P14	NBF	Bx	110	105	172	112	19	70	NA
P14	NBF	Ctrl	16	2*	31	10	23	<10	NA
P14	NBF	Tu	150	149	192	132	9	80	NA
P14	UMFIX	Bx	92	80	170	21	3	70	NA
P14	UMFIX	Ctrl	6	NA	81	0	5	<10	NA
P14	UMFIX	Tu	108	120	153	115	5	60	NA
P15	NBF	Bx	2	47	94	5	4	30	0.406
P15	NBF	Ctrl	0	4	24	50	5	<10	NA
P15	NBF	Tu	8	68	80	13	1	40	0.377
P15	SF	Bx	NA	NA	NA	NA	NA	NA	0.622
P15	SF	Tu	NA	NA	NA	NA	NA	NA	0.536
P15	UMFIX	Bx	0	125	119	0	18	50	0.412
P15	UMFIX	Ctrl	0	19	67	17	3	<10	NA
P15	UMFIX	Tu	2	76	87	3	38	50	0.509
P16	NBF	Bx	157	119	139	167	5	NA	0.715
P16	NBF	Ctrl	0	4	16	84*	4	<10	NA
P16	NBF	Tu	186	147*	178	187	0	90	0.908
P16	SF	Bx	NA	NA	NA	NA	NA	NA	0.925
P16	SF	Tu	NA	NA	NA	NA	NA	NA	0.908
P16	UMFIX	Bx	64	26	103	34	15	NA	0.794
P16	UMFIX	Ctrl	0	2	62	NA	3	<10	NA
P16	UMFIX	Tu	148	NA	119	108	3	85	0.881

Supplementary Table 7: REMARK table

Patient ID	Fixation	Tissue	DNA QC	sWGS	TAm-Seq	H&E	IHC-p53	IHC-CK7	IHC-Pax8	IHC-WT1	IHC-CK20
P1	NBF	Ctrl	N	N	N	Y	Y	Y	Y	Y	Y
P1	NBF	Tu	N	N	N	Y	Y	Y	Y	Y	Y
P1	UMFIX	Ctrl	N	N	N	Y	Y	Y	Y	Y	Y
P1	UMFIX	Tu	N	N	N	Y	Y	Y	Y	Y	Y
P2	NBF	Ctrl	N	N	N	Y	Y	Y	Y	Y	Y
P2	NBF	Tu	N	Y	N	Y	Y	Y	Y	Y	Y
P2	SF	Tu	N	Y	N	N	N	N	N	N	N
P2	UMFIX	Ctrl	N	N	N	Y	Y	Y	Y	Y	Y
P2	UMFIX	Tu	N	Y	N	Y	Y	Y	Y	Y	Y
P3	NBF	Bx	Y	Y	Y	Y	Y	Y	Y	Y	Y
P3	NBF	Ctrl	N	N	N	Y	Y	Y	Y	Y	Y
P3	NBF	Tu	Y	Y	Y	Y	Y	Y	Y	Y	Y
P3	SF	Bx	Y	Y	Y	N	N	N	N	N	N
P3	SF	Tu	Y	Y	Y	N	N	N	N	N	N
P3	UMFIX	Bx	Y	Y	Y	Y	Y	Y	Y	Y	Y
P3	UMFIX	Ctrl	N	N	N	Y	Y	Y	Y	Y	Y
P3	UMFIX	Tu	Y	Y	Y	Y	Y	Y	Y	Y	Y
P4	NBF	Bx	Y	Y	Y	Y	Y	Y	Y	Y	N
P4	NBF	Ctrl	N	N	N	Y	Y	Y	Y	Y	N
P4	NBF	Tu	Y	Y	Y	Y	Y	Y	Y	Y	N
P4	SF	Bx	Y	Y	Y	N	N	N	N	N	N

P4	SF	Tu	Y	Y	Y	N	N	N	N	N	N
P4	UMFIX	Bx	Y	Y	Y	Y	Y	Y	Y	Y	N
P4	UMFIX	Ctrl	N	N	N	Y	Y	Y	Y	Y	N
P4	UMFIX	Tu	Y	Y	Y	Y	Y	Y	Y	Y	N
P5	NBF	Bx	Y	Y	Y	Y	Y	Y	Y	Y	Y
P5	NBF	Ctrl	N	N	N	Y	Y	Y	Y	Y	Y
P5	NBF	Tu	Y	Y	Y	Y	Y	Y	Y	Y	Y
P5	SF	Bx	Y	Y	Y	N	N	N	N	N	N
P5	SF	Tu	Y	Y	Y	N	N	N	N	N	N
P5	UMFIX	Bx	Y	Y	Y	Y	Y	Y	Y	Y	Y
P5	UMFIX	Ctrl	N	N	N	Y	Y	Y	Y	Y	Y
P5	UMFIX	Tu	Y	Y	Y	Y	Y	Y	Y	Y	Y
P6	NBF	Bx	Y	Y	Y	Y	Y	Y	N	Y	Y
P6	NBF	Ctrl	N	N	N	Y	Y	Y	Y	Y	Y
P6	NBF	Tu	Y	Y	Y	Y	Y	Y	Y	Y	Y
P6	SF	Bx	Y	Y	Y	N	N	N	N	N	N
P6	SF	Tu	Y	Y	Y	N	N	N	N	N	N
P6	UMFIX	Bx	Y	Y	Y	Y	Y	Y	N	Y	Y
P6	UMFIX	Ctrl	N	N	N	Y	Y	Y	Y	Y	Y
P6	UMFIX	Tu	Y	Y	Y	Y	Y	Y	Y	Y	Y
P7	NBF	Ctrl	N	N	N	Y	Y	Y	Y	Y	Y
P7	NBF	Tu	N	N	N	Y	Y	Y	Y	Y	Y
P7	UMFIX	Ctrl	N	N	N	Y	Y	Y	Y	Y	Y
P7	UMFIX	Tu	N	N	N	Y	Y	Y	Y	Y	Y
P8	NBF	Bx	Y	Y	Y	Y	N	Y	Y	Y	N
P8	NBF	Ctrl	N	N	N	Y	Y	Y	Y	Y	N
P8	NBF	Tu	Y	Y	Y	Y	Y	Y	Y	Y	N
P8	SF	Bx	Y	Y	Y	N	N	N	N	N	N
P8	SF	Tu	Y	Y	Y	N	N	N	N	N	N
P8	UMFIX	Bx	Y	Y	Y	Y	N	Y	Y	Y	N
P8	UMFIX	Ctrl	N	N	N	Y	Y	Y	Y	Y	N
P8	UMFIX	Tu	Y	Y	Y	Y	Y	Y	Y	Y	N
P9	NBF	Bx	N	N	N	Y	Y	Y	Y	Y	Y
P9	NBF	Bx	Y	Y	Y	Y	Y	Y	Y	Y	Y
P9	NBF	Bx	N	N	N	Y	N	N	N	N	N
P9	NBF	Ctrl	N	N	N	Y	Y	Y	Y	Y	Y
P9	NBF	Tu	Y	Y	Y	Y	Y	Y	Y	Y	Y
P9	SF	Bx	Y	Y	Y	N	N	N	N	N	N
P9	SF	Tu	Y	Y	Y	N	N	N	N	N	N
P9	UMFIX	Bx	N	N	N	Y	Y	Y	Y	Y	Y
P9	UMFIX	Bx	Y	Y	Y	Y	Y	Y	Y	Y	Y
P9	UMFIX	Ctrl	N	N	N	Y	Y	Y	Y	Y	Y
P9	UMFIX	Tu	Y	Y	Y	Y	Y	Y	Y	Y	Y
P10	NBF	Ctrl	N	N	N	Y	Y	Y	Y	Y	Y
P10	NBF	Tu	N	N	N	Y	Y	Y	Y	Y	Y
P10	UMFIX	Ctrl	N	N	N	Y	Y	Y	Y	Y	Y
P10	UMFIX	Tu	N	N	N	Y	Y	Y	Y	Y	Y
P11	NBF	Bx	Y	Y	Y	Y	Y	Y	Y	Y	Y
P11	NBF	Ctrl	N	N	N	Y	Y	Y	Y	Y	Y
P11	NBF	Tu	Y	Y	Y	Y	Y	Y	Y	Y	Y
P11	SF	Bx	Y	Y	Y	N	N	N	N	N	N
P11	SF	Tu	Y	Y	Y	N	N	N	N	N	N
P11	UMFIX	Bx	Y	Y	Y	Y	Y	Y	Y	Y	Y
P11	UMFIX	Ctrl	N	N	N	Y	Y	Y	Y	Y	Y
P11	UMFIX	Tu	Y	Y	Y	Y	Y	Y	Y	Y	Y
P12	NBF	Bx	N	N	Y	N	N	N	N	N	N
P12	NBF	Tu	N	N	Y	N	N	N	N	N	N
P12	SF	Bx	N	N	Y	N	N	N	N	N	N
P12	SF	Tu	N	N	Y	N	N	N	N	N	N
P12	UMFIX	Bx	N	N	Y	N	N	N	N	N	N
P12	UMFIX	Tu	N	N	Y	N	N	N	N	N	N
P13	NBF	Bx	Y	Y	Y	Y	Y	Y	Y	Y	Y
P13	NBF	Ctrl	N	N	N	Y	Y	Y	Y	Y	Y
P13	NBF	Tu	Y	Y	Y	Y	Y	Y	Y	Y	Y
P13	SF	Bx	Y	Y	Y	N	N	N	N	N	N
P13	SF	Tu	Y	Y	Y	N	N	N	N	N	N
P13	UMFIX	Bx	Y	Y	Y	Y	Y	Y	Y	Y	Y
P13	UMFIX	Ctrl	N	N	N	Y	Y	Y	Y	Y	Y
P13	UMFIX	Tu	Y	Y	Y	Y	Y	Y	Y	Y	Y
P14	NBF	Bx	Y	Y	N	Y	Y	Y	Y	Y	Y
P14	NBF	Ctrl	N	N	N	Y	Y	N	Y	Y	Y
P14	NBF	Tu	Y	Y	N	Y	Y	Y	Y	Y	Y
P14	NBF	Tu	N	N	N	Y	N	N	N	N	N
P14	SF	Bx	Y	Y	N	N	N	N	N	N	N
P14	SF	Tu	Y	Y	N	N	N	N	N	N	N
P14	UMFIX	Bx	Y	Y	N	Y	Y	Y	Y	Y	Y
P14	UMFIX	Ctrl	N	N	N	Y	Y	N	Y	Y	Y
P14	UMFIX	Tu	Y	Y	N	Y	Y	Y	Y	Y	Y
P15	NBF	Bx	Y	Y	Y	Y	Y	Y	Y	Y	Y
P15	NBF	Ctrl	N	N	N	Y	Y	Y	Y	Y	Y
P15	NBF	Tu	Y	Y	Y	Y	Y	Y	Y	Y	Y
P15	SF	Bx	Y	Y	Y	N	N	N	N	N	N
P15	SF	Tu	Y	Y	Y	N	N	N	N	N	N
P15	UMFIX	Bx	Y	Y	Y	Y	Y	Y	Y	Y	Y
P15	UMFIX	Ctrl	N	N	N	Y	Y	Y	Y	Y	Y
P15	UMFIX	Tu	Y	Y	Y	Y	Y	Y	Y	Y	Y
P15	UMFIX	Tu	N	N	N	Y	N	N	N	N	N
P16	NBF	Bx	Y	Y	Y	Y	Y	Y	Y	Y	Y
P16	NBF	Ctrl	N	N	N	Y	Y	Y	Y	N	Y
P16	NBF	Tu	Y	Y	Y	Y	Y	N	Y	Y	Y
P16	SF	Bx	Y	Y	Y	N	N	N	N	N	N
P16	SF	Tu	Y	Y	Y	N	N	N	N	N	N

P16	UMFIX	Bx	Y	Y	Y	Y	Y	Y	Y	Y	Y
P16	UMFIX	Ctrl	N	N	N	Y	Y	Y	Y	N	Y
P16	UMFIX	Tu	Y	Y	Y	Y	Y	N	Y	Y	Y

References

[1] Ludmil B Alexandrov et al. "Signatures of mutational processes in human cancer." en. In: *Nature* 500.7463 (Aug. 2013), pp. 415–21. ISSN: 1476-4687. DOI: 10.1038/nature12477. URL: http://www.nature.com/nature/journal/vaop/ncurrent/full/nature12477.html?goback=.gde_2130872_member_266007157.

[2] Melissa L. Cox et al. "Assessment of fixatives, fixation, and tissue processing on morphology and RNA integrity". In: *Experimental and Molecular Pathology* 80 (2006), pp. 183–191. ISSN: 00144800. DOI: 10.1016/j.yexmp.2005.10.002.

[3] Mark A DePristo et al. "A framework for variation discovery and genotyping using next-generation DNA sequencing data." In: *Nature genetics* 43.5 (May 2011), pp. 491–8. ISSN: 1546-1718. URL: http://dx.doi.org/10.1038/ng.806.

[4] H. Do and A. Dobrovic. "Sequence Artifacts in DNA from Formalin-Fixed Tissues: Causes and Strategies for Minimization". In: *Clinical Chemistry* 61.1 (2014), pp. 64–71. ISSN: 0009-9147. DOI: 10.1373/clinchem.2014.223040. URL: http://www.clinchem.org/cgi/doi/10.1373/clinchem.2014.223040.

[5] Hongdo Do et al. "Reducing sequence artifacts in amplicon-based massively parallel sequencing of formalin-fixed paraffin-embedded DNA by enzymatic depletion of uracil-containing templates". In: *Clinical Chemistry* 59.9 (2013), pp. 1376–1383. ISSN: 00099147. DOI: 10.1373/clinchem.2012.202390.

[6] Michael P. Douglas and Scott O. Rogers. "DNA damage caused by common cytological fixatives". In: *Mutation Research - Fundamental and Molecular Mechanisms of Mutagenesis* 401.1-2 (1998), pp. 77–88. ISSN: 00275107. DOI: 10.1016/S0027-5107(97)00314-X.

[7] Tim Forshew et al. "Noninvasive identification and monitoring of cancer mutations by targeted deep sequencing of plasma DNA." In: *Science translational medicine* 4.136 (May 2012), 136ra68. ISSN: 1946-6242. DOI: 10.1126/scitranslmed.3003726. URL: http://www.ncbi.nlm.nih.gov/pubmed/22649089.

[8] Julian S. Gehring et al. "SomaticSignatures: Inferring Mutational Signatures from Single Nucleotide Variants". In: *Bioinformatics* (July 2015), btv408. ISSN: 1367-4803. URL: http://bioinformatics.oxfordjournals.org/content/early/2015/08/13/bioinformatics.btv408.

[9] William J Howat and Beverley a Wilson. "Tissue fixation and the effect of molecular fixatives on downstream staining procedures." In: *Methods (San Diego, Calif.)* 70.1 (2014), pp. 12–19. ISSN: 1095-9130. DOI: 10.1016/j.ymeth.2014.01.022. URL: http://www.ncbi.nlm.nih.gov/pubmed/24561827.

[10] Heng Li. "Aligning sequence reads, clone sequences and assembly contigs with BWA-MEM". In: (Mar. 2013), p. 3. URL: http://arxiv.org/abs/1303.3997.

[11] Heng Li et al. "The Sequence Alignment/Map format and SAMtools." In: *Bioinformatics (Oxford, England)* 25.16 (Aug. 2009), pp. 2078–9. ISSN: 1367-4811. URL: http://www.ncbi.nlm.nih.gov/pubmed/19505943.

[12] William McLaren et al. "Deriving the consequences of genomic variants with the Ensembl API and SNP Effect Predictor." In: *Bioinformatics (Oxford, England)* 26.16 (Aug. 2010), pp. 2069–70. ISSN: 1367-4811. URL: http://www.pubmedcentral.nih.gov/articlerender.fcgi?artid=2916720\&tool=pmcentrez\&rendertype=abstract.

[13] Paul Theodor Pyl et al. "h5vc: scalable nucleotide tallies with HDF5." In: *Bioinformatics (Oxford, England)* 30.10 (May 2014), pp. 1464–6. ISSN: 1367-4811. URL: http://bioinformatics.oxfordjournals.org/content/30/10/1464.

[14] Steven A Roberts et al. "An APOBEC cytidine deaminase mutagenesis pattern is widespread in human cancers." en. In: *Nature genetics* 45.9 (Sept. 2013), pp. 970–6. ISSN: 1546-1718. URL: http://www.nature.com/ng/journal/v45/n9/full/ng.2702.html?WT.ec_id=NG-201309.

[15] Ilari Scheinin et al. "DNA copy number analysis of fresh and formalin-fixed specimens by shallow whole-genome sequencing with identification and exclusion of problematic regions in the genome assembly". In: *Genome Research* 24.12 (Dec. 2014), pp. 2022–2032. ISSN: 1088-9051. DOI: 10.1101/gr.175141.114. URL: http://genome.cshlp.org/content/24/12/2022.short.

[16] David H. Spencer et al. "Comparison of clinical targeted next-generation sequence data from formalin-fixed and fresh-frozen tissue specimens". In: *Journal of Molecular Diagnostics* 15.5 (2013), pp. 623–633. ISSN: 15251578. DOI: 10.1016/j.jmoldx.2013.05.004. URL: http://dx.doi.org/10.1016/j.jmoldx.2013.05.004.

[17] Mythily Srinivasan, Daniel Sedmak, and Scott Jewell. "Effect of fixatives and tissue processing on the content and integrity of nucleic acids." In: *The American journal of pathology* 161.6 (2002), pp. 1961–1971. ISSN: 00029440. DOI: 10.1016/S0002-9440(10)64472-0. URL: http://dx.doi.org/10.1016/S0002-9440(10)64472-0.

[18] Helga Thorvaldsdóttir, James T Robinson, and Jill P Mesirov. "Integrative Genomics Viewer (IGV): high-performance genomics data visualization and exploration." In: *Briefings in bioinformatics* 14.2 (Mar. 2013), pp. 178–92. ISSN: 1477-4054. URL: http://bib.oxfordjournals.org/content/14/2/178.full?keytype=ref\&ijkey=qTgjFwbRBAzRZWC.

[19] Gulisa Turashvili et al. "Nucleic acid quantity and quality from paraffin blocks: Defining optimal fixation, processing and DNA/RNA extraction techniques". In: *Experimental and Molecular Pathology* 92.1 (2012), pp. 33–43. ISSN: 00144800. DOI: 10.1016/j.yexmp.2011.09.013. URL: http://dx.doi.org/10.1016/j.yexmp.2011.09.013.

[20] Vladimir Vincek et al. "A tissue fixative that protects macromolecules (DNA, RNA, and protein) and histomorphology in clinical samples." In: *Laboratory investigation; a journal of technical methods and pathology* 83.10 (2003), pp. 1427–1435. ISSN: 0023-6837. DOI: 10.1097/01.LAB.0000090154.55436.D1.

[21] C Williams et al. "A high frequency of sequence alterations is due to formalin fixation of archival specimens." In: *The American journal of pathology* 155.5 (1999), pp. 1467–1471. ISSN: 00029440. DOI: 10.1016/S0002-9440(10)65461-2.

[22] V Zsikla, M Baumann, and G Cathomas. "Effect of buffered formalin on amplification of DNA from paraffin wax embedded small biopsies using real-time PCR." In: *Journal of clinical pathology* 57.6 (2004), pp. 654–656. ISSN: 0021-9746. DOI: 10.1136/jcp.2003.013961.